Nonradiative decay dynamics of methyl-4-hydroxycinnamate and its hydrated complex revealed by picosecond pump-probe spectroscopy

Journal:	*Physical Chemistry Chemical Physics*
Manuscript ID:	CP-ART-12-2011-024056.R1
Article Type:	Paper
Date Submitted by the Author:	n/a
Complete List of Authors:	Ebata, TAKAYUKI; Hiroshima University, Chemistry Shimada, Daiki; Hiroshima University, Chemistry Kusaka, Ryoji; Hiroshima University, Chemistry Inokuchi, Yoshiya; Hiroshima University, Chemistry Ehara, Masahiro; Institute for Molecular Science,

Nonradiative decay dynamics of methyl-4-hydroxycinnamate and its hydrated complex revealed by picosecond pump-probe spectroscopy

Daiki Shimada[1], Ryoji Kusaka[1], Yoshiya Inokuchi[1], Masahiro Ehara[2a)], and Takayuki Ebata[1a)]

[1] Department of Chemistry, Graduate School of Science, Hiroshima University, Higashi-Hiroshima 739-8526, Japan
[2] Institute for Molecular Science, 38 Myodaiji, Okazaki 444-8585, Japan

---

Abstract: The lifetimes of methyl 4-hydroxycinnamate (OM*p*CA) and its mono-hydrated complex (OM*p*CA-H_2O) in the S_1 state have been measured by picosecond pump-probe spectroscopy in a supersonic beam. For OM*p*CA, the lifetime of the S_1 - S_0 origin is 8 – 9 ps. On the other hand, the lifetime of OM*p*CA-H_2O complex at the origin is 930 ps, which is ~100 times longer than that. Furthermore, in the complex the S_1 lifetime shows rapid decrease at an energy of ~200 cm^{-1} above the origin and finally becomes as short as 9 ps at ~500 cm^{-1}. Theoretical calculations with symmetry-adapted cluster-configuration interaction (SAC-CI) method suggest that the observed lifetime behavior of the two species is described by noradiative decay dynamics involving *trans*→*cis* isomerization. That is both OM*p*CA and OM*p*CA-H_2O in the S_1 sate decay due to the *trans*→*cis* isomerization, and the large difference of the lifetimes between them is due to the difference of the isomerization potential energy curve. In OM*p*CA, the *trans*→*cis* isomerization occurs smoothly without a barrier on the S_1 surface, while in OM*p*CA-H_2O complex, there exists a barrier along the isomerization coordinate. The calculated barrier height of OM*p*CA-H_2O is in good agreement with that observed experimentally.

---

a) Authors to whom correspondence should be addressed. Electronic addresses: tebata@hiroshima-u.ac.jp and ehara@ims.ac.jp

Introduction

Methyl 4-hydroxycinnamate (OM*p*CA) has been studied as a model of chromophore of Photoactive Yellow Protein (PYP), a cytoplasmic photoreceptor protein, found in the Halorhodospira halophila bacterium.[1-2] The photocycle of PYP is initiated by the photoinduced *trans*→*cis* isomerization of the *para*-coumaric acid (*p*CA) chromophore (**scheme 1**), which is bridged to a cysteine residue of the protein by a thio-ester bond. In addition, cinnamate derivatives are widely used as ultraviolet B (UVB) blocking compounds in cosmetic sunscreen agents.[3-5] In both cases, the chromophores undergo efficient nonradiative relaxation process involving *trans*→*cis* isomerization from the photoexcited $S_1(\pi\pi^*)$ state. However, the detailed dynamics of this nonradiative process is not yet fully understood. From experimental and theoretical studies, it has been suggested that several electronic states might be involved in this process. Theoretical calculations predict two electronic excited states nearby the $S_1(\pi\pi^*)$ state, e.g. $S_2(\pi\pi^*)$ and $S_3(n\pi^*)$.[6-8] The energy levels of all the states are very sensitive to the surrounding environment and substituents bound to the chromophore,[9] which results in the complexity and difficulty to analyze the observed results related to the photoinduced isomerization dynamics of *p*CA.

Understanding the effect of hydrogen(H)-bonding on the nonradiative dynamics has been of particular interest. For example, the S_1 lifetime of phenol increases by a factor of four upon the H-bonding with water.[10,11] In PYP, its phenolic OH group is H-bonded to tyrosine and glutamic acid, and this H-bonding is thought to influence the nonradiative dynamics of the S_1 state. Very recently, high-resolution spectroscopic studies of *p*CA and OM*p*CA in gas phase have been carried out by Buma and coworkers.[8,12] They measured the S_1-S_0 electronic spectra of OM*p*CA and OM*p*CA-H_2O complex in a supersonic free jet. They estimated the lifetimes of OM*p*CA-H_2O at the S_1 band origin, and reported the lifetime of OM*p*CA-H_2O is two orders of magnitudes longer than that of OM*p*CA.[12] They interpreted the difference in S_1 lifetime to be due to the difference of the nonradiative decay rateto the nπ* state. However, the contribution of the nπ* state is not clear. In this respect, more detailed information of the S_1 lifetime, such as time prrofile as well as the energy dependence, is essential to study the potential crossing and barrier height of the isomerization. Moreover, a higher-level theoretical calculation of the potential energy surface along the isomerization coordinate is necessary.

In the present work, the lifetimes of the S_1 state were measured for OM*p*CA and OM*p*CA-H_2O by picosecond UV-UV pump-probe spectroscopy in a supersonic beam. The obtained S_1 lifetime of OM*p*CA in its band origin is 8 - 9 ps, while that of OM*p*CA-H_2O is 930 ps. Furthermore, the lifetime of the complex remarkably shortens with the energy and becomes as short as 9 ps at ~ 500cm^{-1} above the origin. We discuss this energy dependence with the results of the *ab initio* calculation at the symmetry-adapted cluster-configuration interaction (SAC-CI) level.

Experimental

The supersonic jet of OMpCA was generated by an adiabatic expansion of a mixture of sample vapor and carrier gas into vacuum. Solid powder of OM*p*CA was heated to 170 ℃ in a sample housing attached at the top of a pulsed valve (General valve series 9). The vapor was mixed with neon carrier at the total pressure of 2 bar, and was expanded into a vacuum chamber through an orifice with 1 mm diameter. For generating OM*p*CA-H_2O complex, a water/neon mixture was used as carrier gas. The molecular beam was obtained by skimming the center of the expansion. The setup of the picosecond laser system has been described in detail elsewhere.[13,14] Briefly, two tunable picosecond UV laser pulses were obtained by second harmonic generation of two optical parametric generation/optical parametric amplifier (OPG/OPA) systems (Ekspra PG401 SH) pumped by a mode-locked picosecond Nd:YAG laser (Ekspra PL2143S). The spectral resolution of the UV laser was 5 cm^{-1} and the time resolutions of two lasers were estimated to be 12 ps.

Two lasers crossed the molecular beam in the vacuum chamber in a counter-propagated manner, and ionized OM*p*CA and OM*p*CA-H_2O in the molecular beam by resonant two-photon ionization (R2PI). The ions were mass-analyzed with a 50 cm time-of-flight tube and were detected by a channeltron (Burle 4900). The electronic spectra were obtained by scanning the UV laser frequency while monitoring the mass-selected ion signals. The decay time profiles of the S_1 state were obtained by measuring pump-probe ion signals as a function of the delay time between the pump UV and probe UV' laser pulses. The delay time was controlled with an optical delay line. The ion signals were processed by a boxcar integrator (Par model 4401/4420) connected by a personal computer. The decay time constants were obtained by convoluting the time profiles by using Gaussian functions with 12 ps pulse width for the two laser pulses. The time constants and intensity ratio of the two components when the decay profile exhibits a double exponential decay were determined by the least-square-method. For the lifetime shorter than the laser pulse width (12ps), the uncertainty was estimated to be ± 3 ps.

Theoretical calculation

Ab initio calculations for the geometry optimization and the potential energy curves were performed by the SAC-CI method.[15-18] The basis set was valence double zeta plus one d-type polarization function (VDZP) of Huzinaga-Dunning [3s2p1d/2s].[19] In the SAC–CI calculations, 1s orbitals of the first-row elements were frozen as cores and all the other electrons were correlated without frozen virtual orbitals. The direct algorithm of the SAC–CI singles and doubles–R (SD–R) variational method[20] was adopted. The direct SAC–CI method calculates all the product terms of S_2S_2, S_2R_1, and S_2R_2 without selection, where S_2 denotes linked double operators in SAC and R_1 and R_2 are linked single and double operators in SAC–CI, respectively. To reduce the computational efforts, the perturbation selection scheme[21] was adopted in Level Two accuracy, namely, $\lambda_g = 5.0 \times 10^{-6}$ and $\lambda_e = 5.0 \times 10^{-7}$ for selecting important doubles. The geometry optimizations of the ππ* and nπ* excited states were performed by the analytical energy gradients of the SAC-CI method, though the vibrational analysis was not carried out at the stationary points. The potential energy curves along the torsion angle were examined in two cases. In the first case, the potential energy curves were calculated by the SAC-CI method, where dihedral angles of C-C=C-C (propenyl unit) were varied with all the other coordinates being fixed to the optimized values for the S_1 state. In the second case, the partial geometry optimization in the ground state was performed with the fixed dihedral angle of C-C=C-C (propenyl unit) and all the other coordinates being optimized (B3LYP/6-311G*). At these geometries, the excited states were calculated by the SAC-CI method with the VDZP basis set, [3s2p1d/2s]. To obtain the smooth potential energy curves along the torsion angle, the second-order approximation of the SAC method[22] was adopted without perturbation selection, which is equivalent to the MP2 calculation. The SAC/SAC–CI calculations were carried out using the Gaussian09 suite of programs, Revision B.01.[23]

Results and discussion

Since *trans*-isomer is more stable than *cis*-isomer in OM*p*CA in S_0, we can presume that OM*p*CA has a *trans*-from initially. However, it is necessary to mention the possible conformers of *trans*-OM*p*CA as shown in Figure 1. These conformers are specified by the combination of *syn*/*anti* orientation of the phenolic OH group and the s-*cis*/s-*trans* configuration of the ester with respect to the propenyl C-C single bond. For OMpCA-H_2O (lower panel of Fig. 1), Smolarek et al. assigned that it has a structure in which phenolic OH is hydrogen-bonded to H_2O as a donor.[12]

Figures 2(a) and (b) show the mass-resolved one-color R2PI spectra of the S_1-S_0 transition of OM*p*CA and OMpCA-H_2O, respectively, obtained by using nanosecond (blue) and picosecond (red) laser systems. The inset in each figure displays the TOF mass spectrum under the condition of R2PI spectral measurement. Each TOF spectrum shows that only the monitored species is selectively generated without forming higher size clusters. The electronic transitions of the four conformers of OM*p*CA are identified by Buma and coworkers.[8,12] The S_1-S_0 band origins of s-*cis* and s-*trans* forms of OM*p*CA are located at 32707 and 32872 cm^{-1}, respectively, which are separated by 165 cm^{-1}. Each band is further separated to the transitions due to the *syn* and *anti* conformers with a separation of less than 5 cm^{-1}. For OM*p*CA-H_2O, the S_1-S_0 band origins of s-*trans* and s-*cis* isomers are assigned to be 32069 and 32133 cm^{-1}, respectively.[12] Similar to OM*p*CA, the separation of the transitions of *syn* and *anti*-conformers is very small. By comparing the nanosecond and picosecond laser R2PI spectra of OMpCA-H_2O in Fig. 2, we see the spectrum with the nanosecond laser is sharper than that of the picosecond laser, since the spectral resolution of nanosecond laser system (0.2 cm^{-1}) is much higher than that of the picosecond laser system (5cm^{-1}). On the other hand, the R2PI spectrum of OM*p*CA shows a much broader feature than that of OM*p*CA-H_2O even by using the nanosecond laser system. The broader bandwidth of OM*p*CA than OM*p*CA-H_2O can be attributed to a higher rotational temperature of OM_pCA than OM*p*CA-H_2O in the molecular beam, and to the shorter S_1 lifetime of OM*p*CA as was reported by Smolarek et al.[12]

We first observed ionization potential (IP_0) of OM*p*CA by picosecond pump-probe spectroscopy to determine appropriate frequency of the probe (ionization) laser for the pump-probe measurement. We followed the same experimental procedure done by Smalarek et al.[12] but by using the picosecond laser system. The pump laser frequency (ν_1) was fixed at the S_1 band origin (32707 cm^{-1}) and the probe laser frequency(ν_2) was scanned over certain range with delay time between the two laser pulses being set at 10 ps. Figure 2(c) shows the observed two-color ionization spectrum. In spite of low ionization efficiency from the S_1 state due to the short lifetime, the ionization spectrum in Fig. 1(c) clearly shows step-like structure at $h\nu_{total}$ = 65020 cm^{-1}, which corresponds to the ionization potential of 8.06 eV. This value is ~60 cm^{-1} higher than that reported by Smolarek et al.[12] At present, we do not have a clear description of this difference. The ionization potential (IP_0) of OM*p*CA-H_2O is reported to be 61395 cm^{-1}. [12] In the present measurement, we fixed the ionization laser frequency at 32590 cm^{-1} for OM*p*CA and at 31790 cm^{-1} for OMpCA-H_2O. These frequencies are high enough to ionize both species from S_1.

Figures 3(a) and (b) show the pump-probe time profiles of s-*cis* and s-*trans* conformers of OM*p*CA at the band origin, respectively. By fitting the time profiles with a single exponential decay, the lifetimes of s-*cis* and s-*trans* conformers at the band origin were determined to be 8 ps and 9 ps with uncertainty of ± 3 ps, respectively. These lifetimes are compared with those reported by Smolarek et al.[12] They estimated the S_1 lifetime for *syn*- and *anti*-conformers of the s-*cis* form as 1.0 and 1.8 ps, respectively from the bandwidth measurements. As already mentioned above, the *syn*/*anti* conformers are indistinguishable, so that our value is only compared to the longer lifetime. Their reported lifetime (1.8 ps) is 4 times shorter than our obtained lifetime. The shorter lifetimes estimated from the bandwidth measurements may come from the contribution of the inhomogeneous broadening, that is the vibronic bands contain several rotational lines even if under the jet-cooled condition, so one cannot extract purely the homogeneous broadening from the rotational contour of the vibronic band. Thus, the homogeneous widths would be narrower and the lifetimes will be longer than their estimated ones. On the other hand, the lifetimes obtained by the direct measurement will be more reliable.

The lifetime of the s-*trans* OM*p*CA-H_2O complex at S_1 origin is remarkably long compared to bare OM*p*CA as seen in Fig. 3(c). By fitting with a single exponential decay, the lifetimes of the s-*cis* and s-*trans* conformers of OM*p*CA-H_2O at the band origin are obtained as 930 ps and 700 ps, respectively. Thus, the S_1 lifetime increases by two orders of magnitudes when the phenolic OH is H-bonded with a single water molecules. As seen in Figs. 3(c) - (f), the time profile dramatically changes with an excess excitation energy. So, we describe the characteristic of the time-profiles by dividing the examined energy into three regions. Here, we define E_{excess} as an excess energy from the band origin of the s-*trans* conformer, that is $E_{\mathrm{exc}} = E - S_1(0,0)_{\text{s-}trans}$.

Region 1: E = 32070 - 32300 cm^{-1} (E_{excess} = 0 - 210 cm^{-1}) The time profiles of the vibronic bands show a single exponential decay with the a lifetime of 700 - 1200 ps.

Region 2 : E = 32330 -32650 cm^{-1} (E_{excess} = 260 - 580 cm^{-1}) The time profiles of the vibronic bands in this region exhibit a double exponential decay expressed by

$$I(t) = A_1 e^{-t/\tau_1} + A_2 e^{-t/\tau_2} \quad . \qquad (1)$$

The lifetime of the fast component rapidly becomes short within narrow energy range region.

Region 3: $E \geq$ 32700 cm^{-1}, ($E_{\mathrm{excess}} \geq$ 630 cm^{-1}). Only the fast component is seen and its lifetime in these region is estimated to be equal to or faster than 8 ps.

The obtained lifetimes of the vibronic bands of OM*p*CA-H_2O are listed in Table 1. For a better understanding of the excess energy dependence of the S_1 lifetime of OM*p*CA-H_2O, we plotted the decay rate constants, $k_1(= \tau_1^{-1})$ and $k_2(= \tau_2^{-1})$, against E_{excess} in Figure 4(a). The decay profile becomes double at $E_{\mathrm{excess}} \geq 200\mathrm{cm}^{-1}$, and the rate constant of the fast component rapidly increases with the energy while that of the slow component shows a gradual increase. The reason of the double exponential decay in the region E_{excess} =

200-600 cm^{-1} is due to the presence of the s-*trans* and s-*cis* conformers of OM*p*CA-H_2O. The band origins of the s-*trans* and s-*cis* are located at 32069 and 32133 cm^{-1} respectively[12], and the relative intensities of vibronic bands of the two conformers are almost equal in the R2PI spectrum of OM*p*CA-H_2O as seen in Fig. 2(b). Actually, we calculated the relative energy of the two conformers at the level of M06-2X/6-31++G**, and found that the s-*cis* conformer is only 280 cm^{-1} more stable than the s-*trans*-conformer. Thus, we plotted the decay rate constants for the two conformers by different colors in Fig. 3, red circle for s-*trans* and blue circle for s-*cis*. By taking into account the presence of the two isomers, we see that **there exists a clear threshold for opening the nonradiative channel** for each conformer. That is, the decay rate constant remarkably rises at ~400 cm^{-1} and 530 cm^{-1} for s-*trans* and s-*cis* conformer, respectively. The S_1 decay constant becomes larger than 1.2 x 10^{11} s^{-1} (corresponding to the lifetime of 8 ps) above these energies, which are too short to be obtained with the present laser system.

Now, we discuss the dynamics of the nonradiative process of the S_1 state of OM*p*CA and OM*p*CA-H_2O based on the experimental results and *ab initio* calculation. We compare two different possibilities. One is the nonradiative decay channel to low lying excited state(s). *Ab initio* calculations by Gromov et al.[7] predicted two electronic states nearby the S_1 ($^1A'$, ππ*) electronic state; the second ππ* state ($^1A'$) and the nπ* state ($^1A''$). We use labelings V' and V for the two ππ*states as denoted by Gromov et al.[7] The V' state arises from "HOMO → LUMO+1" transition and the V state from "HOMO → LUMO" transition. The V' state corresponds to the S_1($^1A'$, ππ*) state. According to the EOM-CCSD calculation,[7] the $^1A''$ (nπ*) state is located higher than the V' state at the optimized geometry of the S_0 ($^1A'$) ground state, but it becomes the lowest excited state and the V' and V states are interchanged when the structure is optimized at the $^1A''$ (nπ*) equilibrium geometry. Thus, the S_1($^1A'$) state may relax to the $^1A''$ (nπ*) state through an intersection of the potential energy curves. Buma and coworkers supported this possibility.[12] If it is the case, the observed increase of the S_1 lifetime of the OM*p*CA-H_2O complex indicates that the energy difference of the potential minima between $S_1(^1A', \pi\pi^*)$ and $^1A''$ ($n\pi^*$) in the OMpCA-H_2O complex should be smaller than in OM*p*CA. To examine this possibility we calculated the energies of the $S_1(^1A')$ and $^1A''$ ($n\pi^*$) states of the OM*p*CA and OM*p*CA-H_2O complex at their optimized geometries by the SAC-CI calculation. The estimated energy difference between the potential minima of these two states is 0.048 eV for OM*p*CA, while it amounts 0.111 eV for the OM*p*CA-H_2O complex, which is opposite to the above prediction. Thus the results suggest that the relaxation to the $n\pi^*$ state cannot explain the present experimental results. It should be also noted that the geometry relaxation of the $n\pi^*$ state is relatively localized in the propenyl unit, while that in the $\pi\pi^*$ state is delocalized over the entire molecule.

The other possibility of the nonradiative process is the direct *trans* → *cis* isomerization on the $S_1(^1A', \pi\pi^*)$ potential energy surface (PES). Figure 5 shows the SAC-CI calculated potential energy curves of the ground and three excited states along the dihedral angle of propenyl double bond. Here the initial geometry of OM*p*CA is *trans* with the dihedral angle of 180 degrees. Since the picosecond UV laser pulse excites OM*p*CA and OM*p*CA-H_2O to the vibronic levels of the S_1 state, the *trans* → *cis* isomerization occurs on the S_1 potential energy surface. So, we obtained the excited state potential energy curves with varying the dihedral angle, where the optimization was performed for the S_1 state. As seen in Fig. 5, we do not see any strong interaction between the $S_1(^1A', \pi\pi^*)$ state and other excited states under this condition. Note that the n and π orbitals intermix to each other along the torsion. As seen in the upper panel of Fig. 5, the energy of the $S_1(^1A', \pi\pi^*)$ state of OM*p*CA smoothly decreases from the *trans* to *cis* forms. In the region of dihedral angle of 180-120°, the single reference SAC is still valid and the calculated energies are reliable. Then, the *trans* → *cis* isomerization will proceed through the conical intersection between S_1 and S_0 at ~90° although the calculation has not been performed to that region. On the other hand, on the S_1 potential curve of the OM*p*CA-H_2O complex there is a barrier with a height of 200 cm^{-1} at the dihedral angle of 165°. Thus, the *trans* → *cis* isomerization rate constants will dramatically change in the energy region of the barrier. The experimentally obtained value of the barrier height is 400 -530 cm^{-1}.

We also examined the other limit of the reaction pathways, where the *trans* → *cis* photo-isomerization occurs starting from the initial geometry same with the S_0 ground state. In this case, we calculated the potential energy curves as a function of the dihedral angle with optimizing all the other coordinates in the S_0 state. The calculated potential energy curves of OM*p*CA and OM*p*CA-H_2O in this condition are shown in Fig. 6. The trend of the potential energy curves of the S_1 state is similar to those calculated for the case where the isomerization occurs in the relaxed geometry in the S_1 state (Fig. 5). Namely, the energy of the S_1 state of OM*p*CA smoothly stabilizes from the *trans* to *cis* forms, while that of OM*p*CA-H_2O has an energy barrier of 1200 cm^{-1}. This result also supports the experimental observation, although the energy barrier is much higher than the other limit.

It should be emphasized that this barrier along the *trans* - *cis* coordinate on the S_1 potential curve could not be obtained by CIS or DFT calculation, although the trend of the curves in OM*p*CA and OMpCA-H_2O system was similar in both methods, namely the curve sharply decreases along the isomerization coordinate in OM*p*CA compared to that in OM*p*CA-H_2O. Thus, the electron correlation seems to be important for this barrier. For more detailed understanding of the energetics and dynamics of photo-excited OM*p*CA and the effect of H-bonding, similar study of the H-bonded complexes with different H - bond strength is necessary, such as OM*p*CA-NH_3. Also, time-resolved photoelectron spectroscopy will give us the information of the electronic states involved in this nonradiative process.

Acknowledgement

T.E. acknowledges the Ministry of Education, Culture, Sports, Science, and Technology (MEXT) for the support through a Grant-in-Aid for the Scientific Research on Priority Area "Molecular Science for Supra Functional Systems" (No. 477). M.E. thanks Dr. K. Bobuatong for the part of the calculations. M.E. acknowledges the supported by JST–CREST, a Grant–in–Aid for Scientific Research from the Japanese Society for the Promotion of Science (JSPS) and the Ministry of Education, Culture, Sports, Science and Technology (MEXT) of Japan. The computations were partly performed using the Research Center for Computational Science in Okazaki, Japan.

References

(1) Sprenger, W. W.; Hoff, W. D.; Armitage, J. P.; Hellingwerf, K. J. *J. Bacteriol.* **1993**, *175*, 3096-3104.

(2) Hellingwerf, K. J.; Hendrikis, J.; Gensch, T. *J. Phys. Chem. A* **2003**, *107*, 1082-1094.

(3) Oriol, L.; Pinol, M.; Serrano, J. L.; Tejedor, R. M. *J. Photochem. Photobiol. A*, **2003**, *155*, 37-45.

(4) Monhaphol, T.; Albinsson, B.; Pattanaargson, S. *J. Pharm. Pharamacol.* **2007**, *59*, 279-288.

(5) Promkatkaew, M.; Suramitr, S.; Karpkird, T. M.; Namuangruk, S.; Ehara, M.; Hannongbua, S. *J. Chem. Phys.* **2009**,*131*, 224306(10 pages).

(6) Changenet-Barret, P.; Espangne, A.; Charier, S.; Baudin, J. –B.; Jullen, L.; Plaza, P.; Hellingwerf, K. J.; Martin, M. M. *Photochem. Photobiolo. Sci.* **2004**, *8*, 823-829.

(7) Gromov, E. V.; Burghardt, I.; Koppel, H.; Cederbaum, L. S. *J. Phys. Chem. A* **2005**, *109*, 4623-4631.

(8) de Groot , M.; Gromov E. V.; Koppel, H.; Buma, W. J. *J. Phys. Chem. B* **2008**,*112*, 4427-4434.

(9) Mataga, N.; Chosrowjan, H.; Taniguchi, S.; Hamada, N.; Tokunaga, F.; Imamoto, Y.; Kataoka, M. *Phys. Chem. Chem. Phys.* **2003**, *5*, 2454-2460.

(10) Lipert, R. ; Bermudez, G.; Colson, S. D. *J. Phys. Chem.* 1988, 92, 3801

(11) Lipert, R. ; Colson, S. D. *J. Phys. Chem.* 1989, 93, 135

(12) Smolarek, S.; Vdovin, A.; Tan, E. M. M.; de Groot, M.; Buma, W. J. J. *Phys. Chem. Chem. Phys.* **2011**, *13* , 4393-4399.

(13) Yamada, Y.; Mikami, N.; Ebata, T. *Proc. Natl. Acad. Sci. U.S.A.* **2008**,*105*,12690-12695.

(14) Kusaka, R.; Ebata, T. *Angew. Chem. Int. Ed.* **2010**, *49*, 6989-6992.

(15) Nakatsuji, H.; Hirao, K. *J. Chem. Phys.* **1978**, 68, 2053-2065.

(16) Nakatsuji, H. *Chem. Phys. Lett.* **1978**, 59, 362-364; Nakatsuji, H. *Chem. Phys. Lett.* **1979**, 67, 329-333.

(17) Nakatsuji, H. *Acta Chim. Acad. Sci. Hung.* **1992**, 129, 719.

(18) Ehara, M.; Hasegawa, J.; Nakatsuji, H. *SAC-CI Method Applied to Molecular Spectroscopy, in Theory and Applications of Computational Chemistry: The First 40 Years, A Volume of Technical and Historical Perspectives.* **2005**, pp. 1099-1141 (Elsevier, Oxford).

(19) Dunning, JR., T. H. *J. Chem. Phys.* **1970**, 53, 2823-2833.

(20) Fukuda, R.; Nakatsuji, H. *J. Chem. Phys.* **2008**, 128, 094105-1-14.

(21) Nakatsuji, H. *Chem. Phys.* **1983**, 75, 425-441.

(22) Nakajima, T.; Nakatsuji, H. *Chem. Phys. Lett.*, **1998**, 300, 1-8.

(23) Frisch, M.J. et al., *GAUSSIAN09 Rev. B.01.* **2010** (Gaussian Inc., Wallingford, CT).

Table 1. Excitation energies (cm^{-1}) and lifetimes (ps) and ratios of the amplitudes of the fast (τ_1) to slow (τ_2) components of the S_1 state of the OMpCA-H_2O complex. See text.

Excitation Energy/cm^{-1}	Excess Energy/cm^{-1}	τ_1 / ps	τ_2 / ps	A_1/A_2
32070	0,0 (s-*trans*)		930 ± 200 [b]	
32130	0,0 (s-*cis*)		700 ± 200 [b]	
32160	90 [a]		1180 ± 300 [b]	
32280	210 [a]		770 ±100 [b]	
32330	260 [a]	45 ± 5	320 ± 100	1
32380	310 [a]	40 ± 10	220 ± 80	1
32440	370 [a]	30 ± 10	220 ± 80	2
32490	420 [a]	≤ 9	210 ±60	3
32540	470 [a]	≤ 9	120 ± 20	2
32590	520 [a]	≤ 9	90 ± 30	4
32650	580 [a]	≤ 9	60 ± 20	6
32700	630 [a]	≤ 9	- [c]	- [c]
32920	850 [a]	9 [d]		

[a] The energies are given with respect to the s-*trans* band origin.

[b] Time profile shows a single exponential decay.

[c] These values cannot determined due to small A_2 coefficient.

[d] Only the short component is observed.

Figure Captions

Figure 1. Schematic structures of four conformers of *trans*-OM*p*CA and the structure of *trans*-OM*p*CA-H_2O.

Figure 2. (a) R2PI spectrum of OMpCA in a supersonic beam. (b) R2PI spectrum of the OMpCA-H2O complex in a supersonic beam. The red-colored spectra are measured by the picosecond laser system and the blue ones by the nanosecond laser system. The insets are the TOF spectra for each measurement. (c) Two-color ionization spectrum of OMpCA, where ν_1 is fixed at band origin of s-*cis* OMpCA (32707 cm^{-1}) and ν_2 is scanned.

Figure 3. Pump-probe time profiles of (a),(b) OMpCA and (c)-(f) OMpCA-H_2O at different excitation energies. The excitation energies and the excess energies (in parentheses) are given. Solid curves are convoluted ones. For the time-profiles of OMpCA and the 0,0 band of OMpCA-H_2O, the decay curves are fitted by a single exponential decay curve, while those of vibronic bands of OMpCA-H_2O are fitted by a double exponential decay curve given by the equation (1).

Figure 4. (upper) Plot of the decay rate constants of the S1 state of OMpCA-H_2O as a function of energy. (lower) R2PI spectrum of the OMpCA-H2O complex in a supersonic beam.

Figure 5. Pontential energy curves of S_0, $S_1(\pi\pi^*)$, $S_2(\pi\pi^*)$ and $S_3(n\pi^*)$ of OMpCA(upper) and OMpCA-H_2O(lower) as a function of the dihedral angle along the propenyl double bond. Here the initial structure is the *trans* with the dihedral angle of 180 degrees. For S_0, the geometry is optimized with the fixed dihedral angle of C-C=C-C (propenyl unit) and all the other coordinates being optimized. For the excited state potential energy curves,

the optimization was performed for the S_1 state and the same geometries are used for other excited states, and the energies are obtained with varying the dihedral angle.

Figure 6. Pontential energy curves of S_0, $S_1(\pi\pi^*)$, $S_2(\pi\pi^*)$ and $S_3(n\pi^*)$ of OMpCA(upper) and OMpCA-H_2O(lower) as a function of the dihedral angle along the propenyl double bond. Here the initial structure is the *trans* with the dihedral angle of 180 degrees. The geometry is optimized for S_0 with the fixed dihedral angle of C-C=C-C (propenyl unit) and all the other coordinates being optimized. The same geometries are used for the excited electronic states.

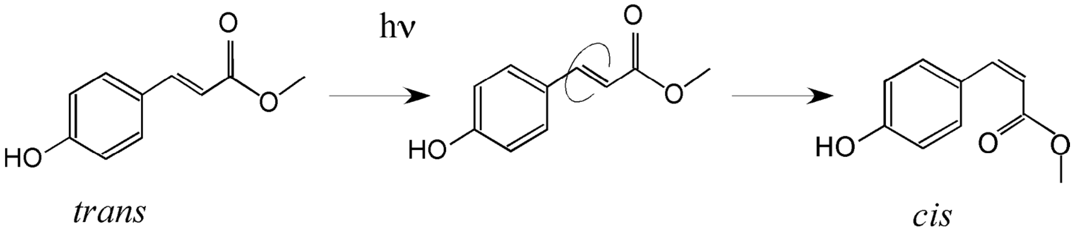

Scheme-1

Fig. 1

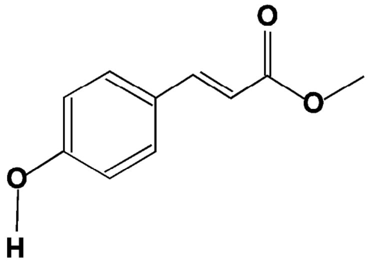

s-cis, OH syn-OMpCA

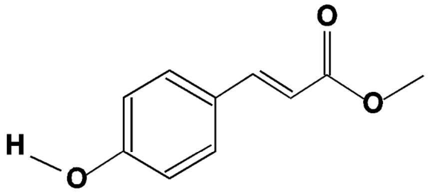

s-cis, OH anti-OMpCA

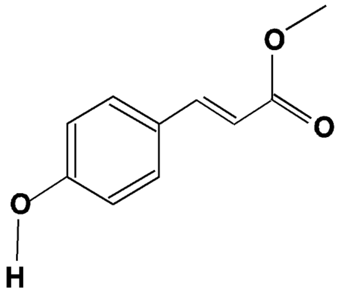

s-trans, OH syn-OMpCA

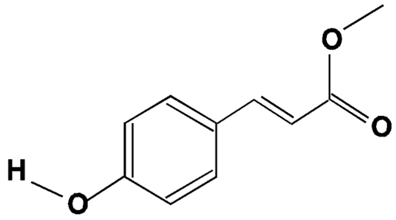

s-trans, OH anti-OMpCA

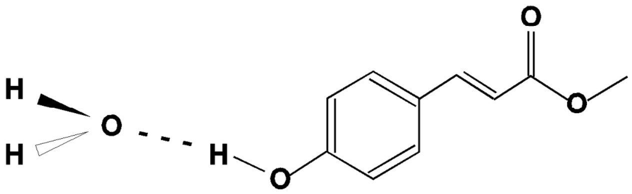

OMpCA-H_2O

Fig. 2

(a) OMpCA

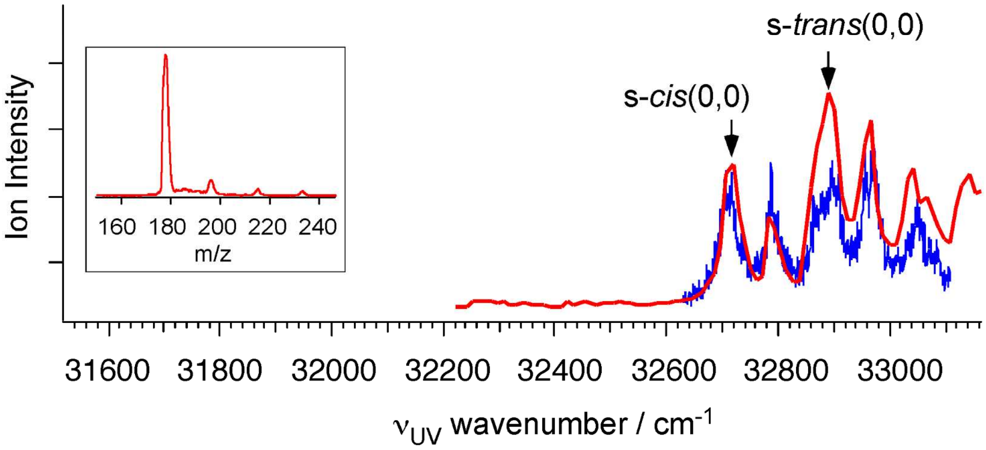

(b) OMpCA-H_2O

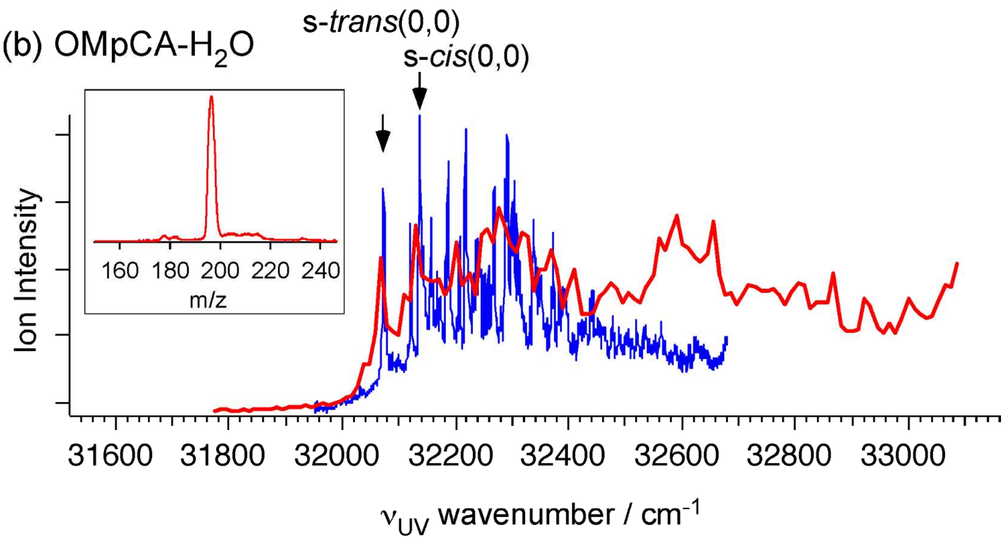

(c) OMpCA

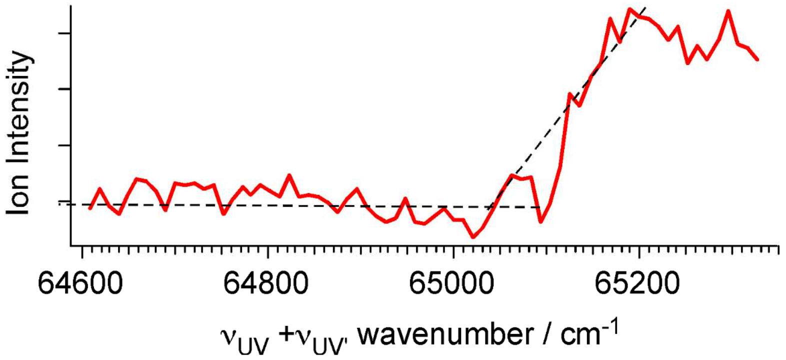

Fig. 3

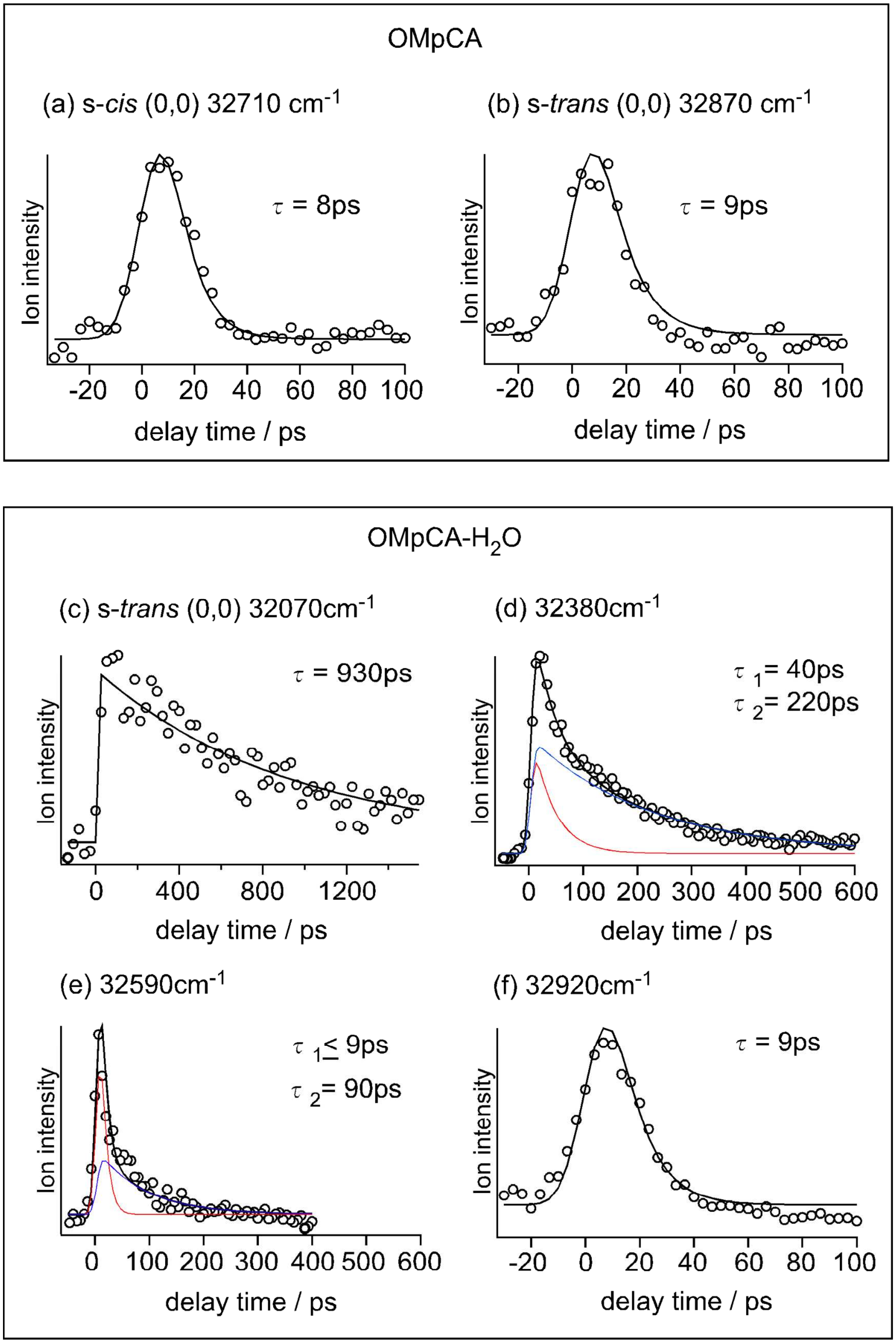
OMpCA
(a) s-*cis* (0,0) 32710 cm^{-1}
(b) s-*trans* (0,0) 32870 cm^{-1}
τ = 8ps
τ = 9ps
Ion intensity
-20 0 20 40 60 80 100
delay time / ps
OMpCA-H_2O
(c) s-*trans* (0,0) 32070cm^{-1}
τ = 930ps
0 400 800 1200
(d) 32380cm^{-1}
τ_1= 40ps
τ_2= 220ps
0 100 200 300 400 500 600
(e) 32590cm^{-1}
$\tau_1 \leq$ 9ps
τ_2= 90ps
(f) 32920cm^{-1}
τ = 9ps
delay time / ps

Fig. 4

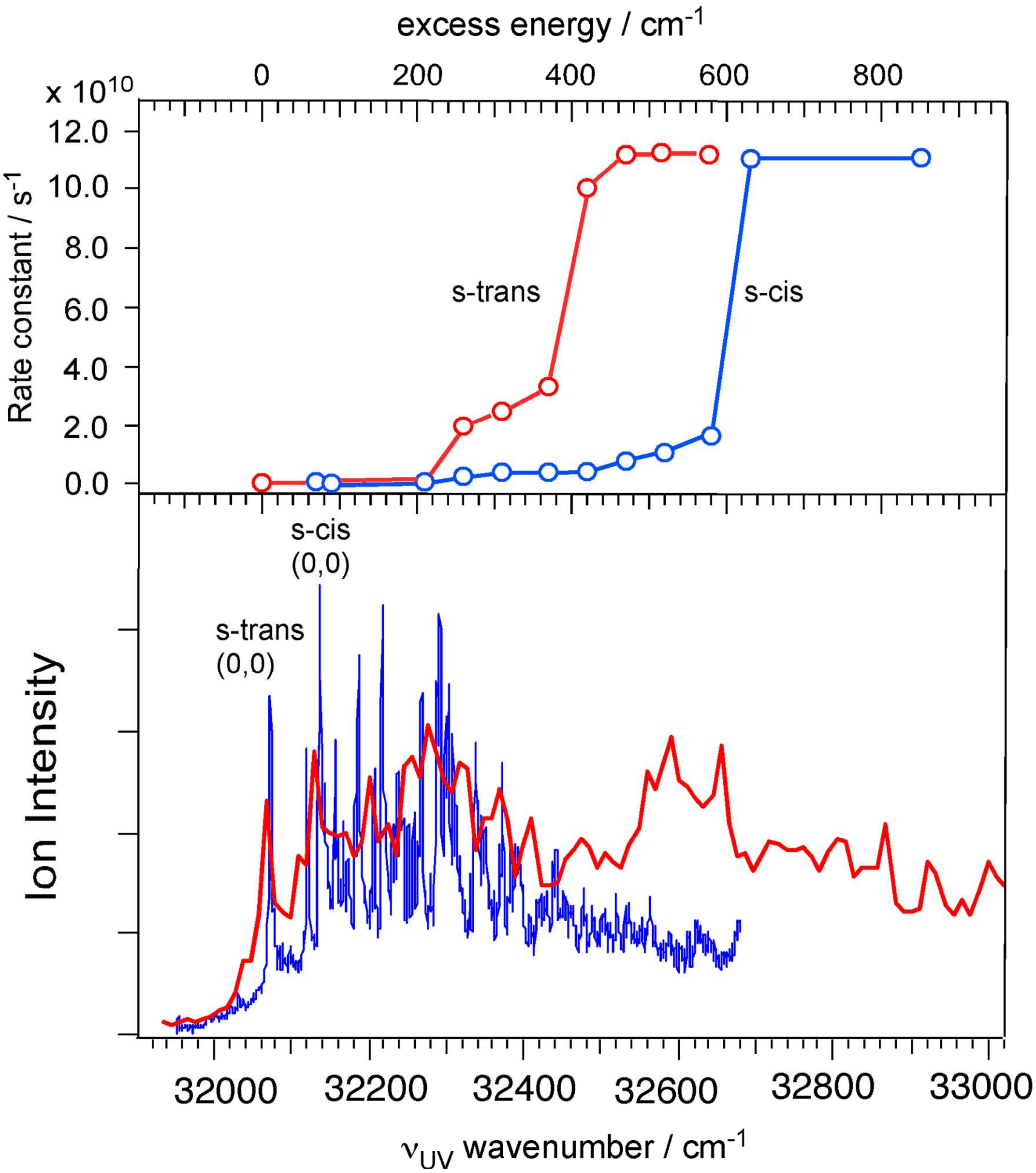
excess energy / cm^{-1}
0
200
400
600
800
x 10^{10}
12.0
10.0
8.0
6.0
4.0
2.0
0.0
Rate constant / s^{-1}
s-trans
s-cis
s-cis (0,0)
s-trans (0,0)
Ion Intensity
32000
32200
32400
32600
32800
33000
ν_{UV} wavenumber / cm^{-1}

Fig. 5

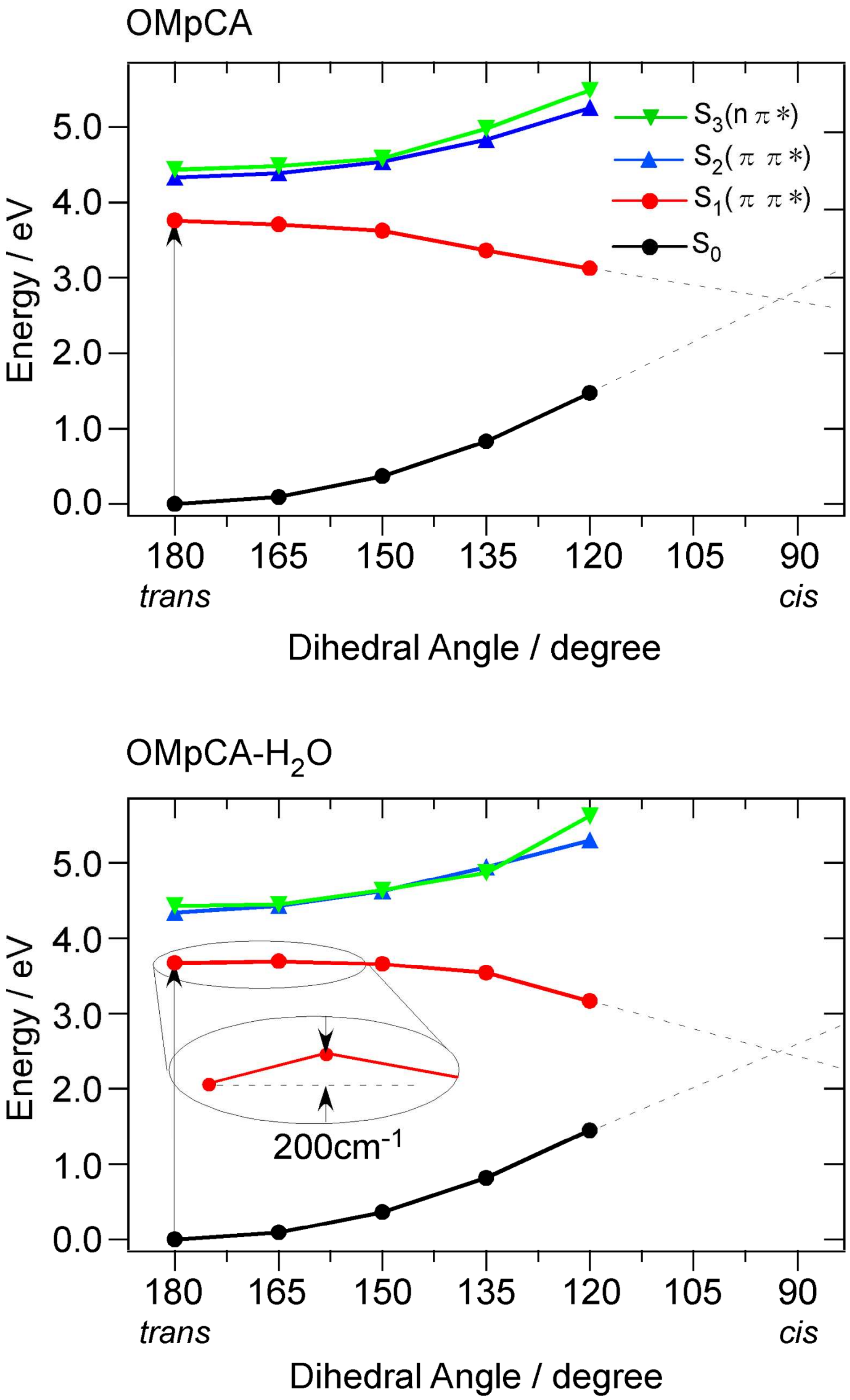

OMpCA

OMpCA-H_2O

Fig. 6

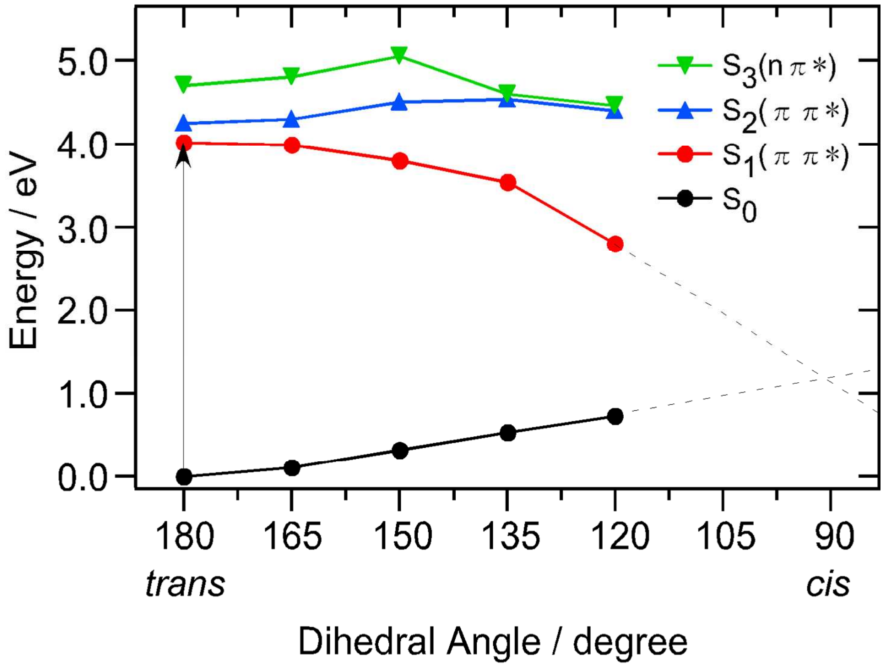

(a) OMpCA

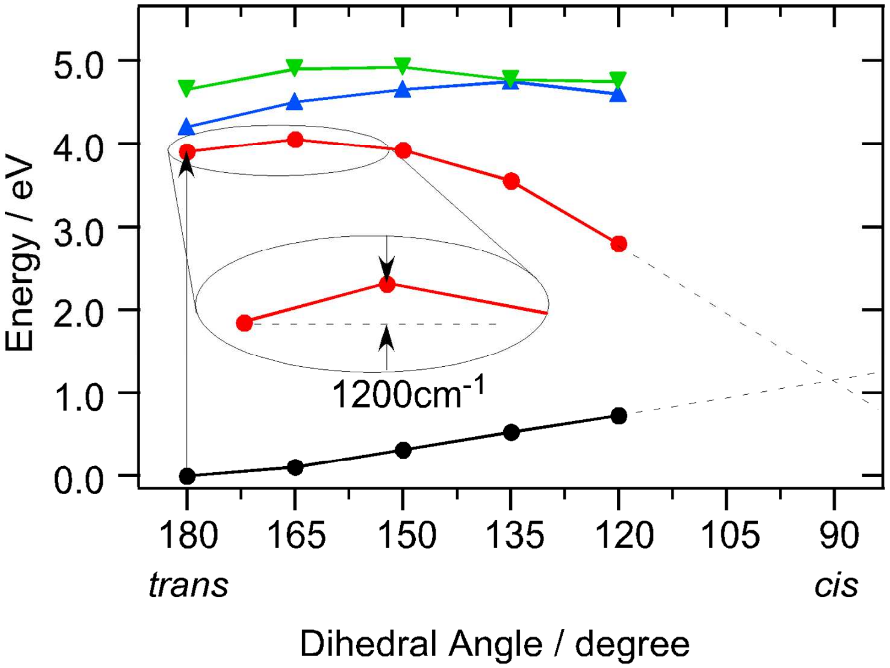

(b) OMpCA-H_2O

Graphic Abstract

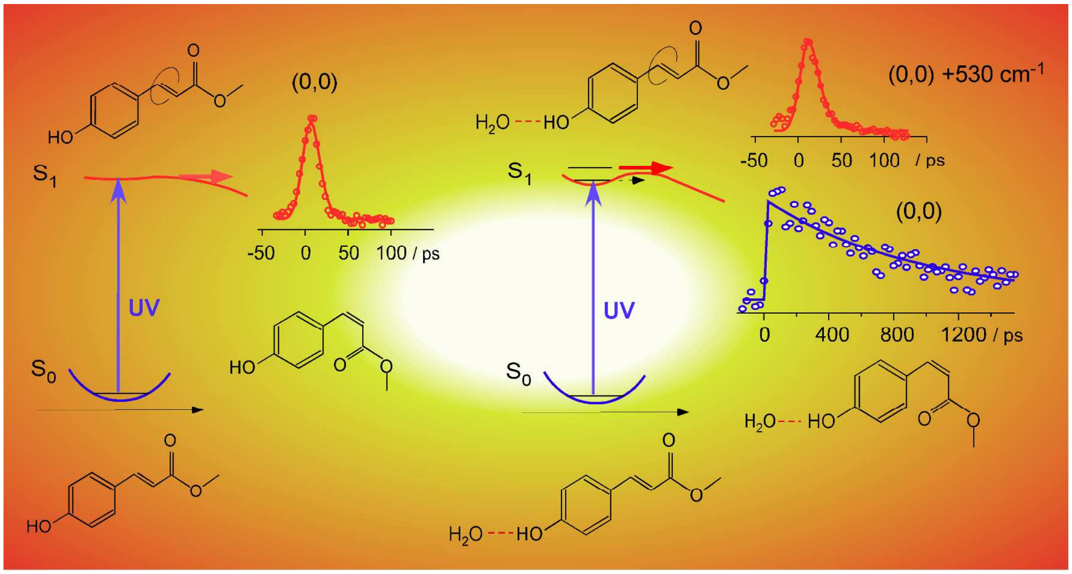

Feb. 18, 2012

Dr. Jane Hordern, Editor
Drs. Guang-Jiu Zhao and Ke-Li Han, Guest Editor
Physical Chemistry Chemical Physics

Dear Editor;

We would like to submit a revised version of our manuscript entitled “**Nonradiative decay dynamics of methyl-4-hydroxycinnamate and its hydrated complex revealed by picosecond pump-probe spectroscopy**“, which is resubmitted to **the themed issue** ”**Hydrogen Bonding in Electronically Excited States**” in **Physical Chemistry Chemical Physics**.

We would like to express our sincere thanks to the referees for their careful checking of our manuscript and for giving pertinent comments. After receiving the review, we reread the text carefully and corrected all grammar and spelling mistakes, as well as incomplete sentences. Additionally, we asked an English editor to check the revised manuscript. Followings are the reply to the reviewers’ comments and the revisions made.

Reviewer 1 Comment

This manuscript reports an interesting and striking result along with a sound interpretation. I believe it should appear in PCCP, but the authors should attend to several points that will make it clearer and more convincing. The critical result is that complexation with a single water molecule changes the lifetime of the excited state by about two orders of magnitude. Increasing the excess energy shortens the lifetime back to near the value for the uncomplexed molecule. The authors attribute this behavior to the presence of a barrier in the complex that is absent in the bare molecule. They support that inference with electronics tructure calculations. There are several points that need attention for clarity or completeness.

(**Comment 1**) There is no discussion of the convolution that must be part of the fitting procedure given the lifetime of 8-9 ps that they infer using 12-ps pulses. The authors should state that they use a convolution with their laser pulse and explain the uncertainties in the fits in Table 1.

(**Reply to the comment and revisions made**) We added the fitting procedure at the end of the experimental section (page 4, lines 10 to 17) as follows,

"The decay time constants were obtained by convoluting the time profiles by using Gaussian functions with 12 ps pulse width for the two laser pulses. The time constants and intensity ratio of the two components when the decay profile exhibits a double exponential decay were determined by the least-square-method. For the lifetime shorter than the laser pulse width (12ps), the uncertainty was estimated to be ± 3 ps."

(**Comment 2**) The discussion on page 9 and 10 of the "geometry relaxation energy" is unclear. It is not apparent what the authors mean by "geometry relaxation energy". Perhaps they mean the difference in the energy of the of the $\pi\pi^*$ and nπ^* minima, but I could not be sure. The authors should explain it.

(**Reply to the comment and revisions made**) As the referee pointed, the "geometry relaxation energy" is close to the meaning to the difference in the energies of the $\pi\pi^*$ and nπ^* minima. However, in the first paper we discussed this part as the difference between the energy at the vertical transition to the $\pi\pi^*$ state and that at the optimized geometry of the nπ^* state. In the revised manuscript, we presented the difference between the energies of the $\pi\pi^*$ and nπ^* minima. Thus, the magnitudes of the energies are smaller than the original one. However, the order of the difference is the same as before. Since this energy difference is crucial in this paper, we recalculated the energies with higher accuracy. We revised this part as follows (page 10, lines 4-9).

"To examine this possibility we calculated the energies of the $S_1(^1A')$ and $^1A''$ (nπ^*) states of the OM*p*CA and OM*p*CA-H_2O complex at their optimized geometries by the SAC-CI calculation. The estimated energy difference between the potential minima of these two states is 0.048 eV for OM*p*CA, while it amounts 0.111 eV for the OM*p*CA-H_2O complex, which is opposite to the above prediction."

(**Comment 3**) Since they have electronic structure calculations available, is it possible to provide a physical explanation of the origin of the barrier in the complex?

(**Reply to the comment and revisions made**) At present, we do not have a clear explanation to answer the question. We also calculated the potential curves using CIS and DFT calculations. But no barrier appeared. It indicates that the electron correlation seems to be important for this barrier. In the revised manuscript, we added the following sentences (page 11, lines 19- 25),

"It should be emphasized that this barrier along the *trans* - *cis* coordinate on the S_1 potential curve could not be obtained by CIS or DFT calculation, although the trend of the curves in OM*p*CA and OMpCA-H_2O system was similar in both methods, namely the curve sharply decreases along the isomerization coordinate in OM*p*CA compared to that in OM*p*CA-H_2O. Thus, the electron correlation seems to be important for this barrier."

(**Comment 4**) The sole figure in the supplementary material should be in the article. It is an important part of the argument.

(**Reply to the comment and revisions made**) We changed it to figure 5.

(**Comment 5**) On page 10, the meaning of "cut of the dihedral angle" is not apparent. The plot in figure only goes to 90o even though they say on page 10 it goes to 180o. It is fine to it only show it to 90o, but they should state it a little differently.

(**Reply to the comment and revisions made**) The meaning of "cut of the dihedral angle" is just along the dihedral angle, with the initial geometry of OM*p*CA is *trans* with the dihedral angle of 180 degrees. We revised this sentence (page 10, lines 15 –18) as follows,

"Figure 5 shows the SAC-CI calculated potential energy curves of the ground and three excited states along the dihedral angle of propenyl double bond. Here the initial geometry of OM*p*CA is *trans* with the dihedral angle of 180 degrees."

(**Other revisions made**)

1. We added a "*trans*→*cis* isomerization scheme" as scheme 1.
2. After receiving the review we reread the text carefully and corrected all grammar and spelling mistakes, as well as incomplete sentences. Additionally, we asked an English editor to check the revised manuscript.

Reviewer 2 Comment

This Manuscript presents a in supersonic beam study of the radiationless decay of the S1 state of OMpCA and of its H-bonded complex with one water molecule. The S1 lifetime of both species is measured by UV pump and probe spectroscopy with a picosecond time resolution. It is found that hydration increases significantly the S1 lifetime when the 0-0 vibrational level is excited, but that the OMpCA lifetime shortens significantly when the excitation energy increases. Ab initio calculations are presented to analyse the experimental results.

Considering the content, this paper can be accepted for publication on PCCP. However, it is not suitable for publication in the present form. There are (these are just examples) incomplete or incorrect words sentences with a verb repeated (4th line of p.4) or missing (18th line of p. 8), with a word missing (4th line from bottom of p.18).

In conclusion, I suggest that the authors read carefully all the paper and improve the text.

(**Revisions made**) After receiving the review we reread the text carefully and corrected all grammar and spelling mistakes, as well as incomplete sentences. Additionally, we asked an English editor to check the revised manuscript.

(**Other revisions made**)

1. We added a "*trans*→*cis* isomerization scheme" as scheme 1.
2. After receiving the review we reread the text carefully and corrected all grammar and spelling mistakes, as well as incomplete sentences. Additionally, we asked an English editor to check the revised manuscript.

We hope the revised manuscript is acceptable for the publication in the Physical Chemistry and Chemical Physics.

Sincerely yours,

Takayuki Ebata
Department of Chemistry,
Graduate School of Science
Hiroshima University, Kagamiyama 1-3-1
Higashi-Hiroshima 739-8526
Fax: 81-82-424-7407
e-mail: tebata@hiroshima-u.ac.jp

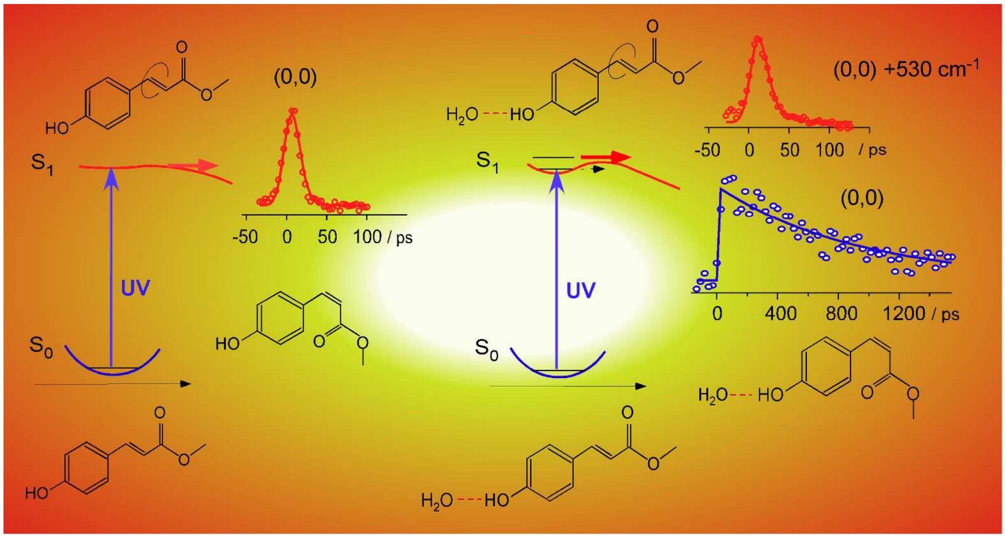

293x155mm (300 x 300 DPI)